Measurements of Visual Binary Stars with a SWIR Camera and a 280 mm Reflector – Part 2

J. Sérot
jocelyn.serot@free.fr

Abstract: This paper is a continuation of that published in [1]. It presents the measurements of visual binary stars obtained by means of an 11" reflector telescope and a VIS-SWIR camera covering the 450 - 1700 nm band. Compared to the results presented in [1] with a similar instrumentation, the observed targets are closer pairs, with separations between 1 and 5 arcsec and reduction was performed using bispectrum-based techniques. Our measurements show a good agreement with astrometric parameters derived from the GAIA DR2. Attempt to correlate the measured differential magnitudes in several bands (450-600 nm, 550-670 nm and 800 - 1700 nm resp.) and the GAIA Teff parameters - viewed as an indirect indicator of the spectral types – did not produce any convincing result.

1. Introduction

In [1], we presented some preliminary results of observation and measurement of visual binary stars with a small telescope and a camera operating in the short wave infrared (SWIR†) band. As a consequence of the target selection process, which focused on stars with late spectral types companions (M, typically), most of results described [1] concern pairs having large separations (in the range 10-100 arcsec typically) and measurements were performed on images obtained by classical select-shift-and-add techniques.

It therefore remained to be investigated whether speckle-based reduction techniques – which we have been using regularly to obtain measurements of close visual binary stars in the optical band [2,3] – could be applied to obtain measurements of closer pairs observed with the same instrumentation.

This was the main motivation of the work described in this paper. The other one was to assess whether measuring the difference in magnitude (ΔM) between the components at different wavelengths could, at least qualitatively, be related to the spectral types of the components.

The paper is organized as follows. Sections 2 and 3 briefly recall the characteristics of our instrumental setup and of the data reduction process. Sections 4 and 5 present the target stars and the related measurements. Section 6 concludes the paper.

† Typically from 1 to 2.5 µm

2. Instrumental setup

As described in [1], the detector is an Owl 640 VIS-SWIR camera manufactored by Raptor Photonics [4]. It features a 640x512 InGaAs PIN-photodiode sensor (15x15 µm pixels), a QE > 80% between 800 and 1600 nm and is equipped with an on-board Non Uniformity Compensation system (NUC) which can perform on the fly offset correction, gain dispersion compensation, dark current substraction and hot pixel correction. The results described here were obtained with the following settings:

- sensor cooled to -15°c
- NUC level 2 (offset + gain correction)
- Hi gain mode, gain = 6-8

Control of the camera and acquisition are carried out by the Genika software (version 2.8.0) [5].

The telescope is a 280 mm Schmidt-Cassegrain reflector (Celestron C11). Because of the relatively large pixels of the camera (15 x 15 µm), and as described in [1], we had to use eyepiece projection to get a plate scale compatible with the measurement of pairs with separation between 1 and 5 arcsec. The effective plate scale, in this experiment was 0.32 arcsec/pixel.

Three filters were used

- ThorLabs FGL-1000M for observing in SWIR
- Astronomik G and R filters from a RGB type IIc set for observing in the optical band.

The combination of the transmission curve of these

Measurements of Visual Binary Stars with a SWIR Camera and a 280 mm Reflector – Part 2

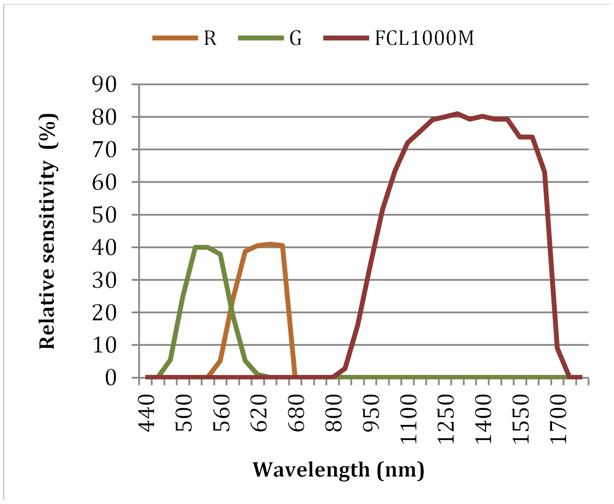

Figure 1. Combined response curve for the Owl 640 camera and the used filters

filters with the QE curve of the Owl 640 gives the relative response curves reproduced in Figure 1. The two following points should be noted. First, despite being a VIS-SWIR camera, the QE of the Owl 640 is significantly lower in the visible part of the spectrum (the QE drops from 90% at λ=1100 nm to 40% at λ=500 nm). This explains the difference in height for the curves associated to the G et R filters on the one side and the FCL-1000M filter on the other side. This difference is not a problem as long as we are interested in *differential* photometry. Second, the sensitivity range in SWIR includes both the J and H photometric bands (1-1.4 and 1.4-1.8 µm resp.). In the sequel of this paper, for brevity, we will refer to the used filters (and corresponding passbands) as "G", "R" and "JH".

3. Acquisition and processing

For each target, seven sequences of 500 frames were acquired:

- one sequence with the G, R and JH filter
- one sequence with the same filters on a nearby reference (single) star, to be used by the deconvolution step in the reduction process,
- one sequence of «dark» frame (obtained with the same gain and exposure time on the sky background).

Individual exposure times ranged from 50 to 75 ms.

Calibration is carried out using the sideral drift method using the dedicated module of the SpeckleToolBox software [6].

All acquired sequences are pre-processed using Reduc [7] and reduced using the bispectrum reconstruction technique supported by the SpeckleToobox software, following the processing pipeline described in [8].

4. Target selection

The selection of potential targets was driven by three criteria:

1. the separation and magnitudes of the components
2. practical observability
3. the possibility to record variations in observed differential magnitudes

The selected range in separation was 1-5 arcsec and the magnitude limit was 10 for the primary and 12 for the secondary. These limits take into account both our goal to measure closer pairs than those reported in [1] and the effective plate scale of approximetly 0.30 arcsec/pixel associated to the instrumental setup (which both limit the resolution and the detectivity of faint stars).

Because observations were performed near the meridian and taking into account the pointing limits in our observatory, the range in RA and Dec were respectively set to 16H-19h and 10-55°.

Our initial idea was, as in [1], to restrict our observations to pairs for which the secondary has a late (M) spectral type. In this case, the variation in Δm according to the observing wavelength is likely to be the most significant. Unfortunately, very few entries in the WDS catalog [9] have a spectral type for the secondary component and virtually none for pairs having a separation under 5 arcsec†. As a workaround, we decided to use the stellar effective temperature parameter (Teff) provided by the GAIA DR2 [10]. Using the GDS tool described in [11], we therefore selected pairs for which both components have a Teff entry in GAIA DR2 and, among these, those for which the difference in Teff was the greatest. This is clearly a very crude filter. First because the Teff parameter is actually inferred from the G, RP and BP photometric data (which do not include J nor H-band photometry). Second because the relationship between the Teff parameter and the spectral type is far from straightforward. But, since our objectives in this experiment were purely qualitative it appeared as an acceptable choice. This left us with a list of 25-30 potential targets, which was far enough.

5. Results

Observations have been conducted during three nights, between 2018-06-26 and 2018-06-30. For each target, and for each filter we had to successively point the target, record a FITS cube, point to a nearby reference star, record a FITS cube and go back to the target

† The only exception in our data set is 18443+3940 (STF2382AB) but it was included in the list only for calibration purposes.

for the next filter. This rather inconvenient way of proceeding was due to the necessity to refocus when changing filters†. As a result, only ten targets were observed.

The observed targets are described in Table 1 and our measurements reported in Table 2.

In Table 1, columns 1-8 respectively give

- the WDS identifier
- the WDS discoverer code
- the position angle (PA) and separation (SEP) computed from the exact coordinates of the components supplied by the GAIA DR2††
- the G magnitude and effective temperature of the two components, as given in the GAIA DR2‡

In Table 2, columns 1-12 respectively give

- the WDS identifier
- the (Besselian) date of the observation
- the measured position angle, separation and differential magnitude (ΔM) when using the G, R and JH filter

The bispectrum-reconstructed images used for the measurements are reproduced in Plate 1.

Two of the measured pairs, BU 627A,BC and STF2382AB have an entry in the Sixth Catalog of Orbits [12]. The O-C computed from our measurement are given in Table 3.

Concerning astrometry (PA and SEP), the measurements in the three observed bands (G, R and JH) are in good agreement. If we except the case of 17344+1310 (A 2184AB), for which the G image is obviously biased, the dispersion between the three values is smaller than 4.3° for PA and 0.33 arcsec for SEP respectively (with a statistical mean of 1.70° and 0.186 arcsec resp.). These dispersions are yet significantly higher than those computed from several measurements of the same pairs in a single, optical, band, as reported in [2] for instance. This can be probably attributed to the much coarser plate scale used here (0.32 arcsec/pixel, compared to 0.09 in [2]) and also to the variability in the quality of the reconstructed images according to the observing wavelength‡‡.

Comparing the measurements obtained in the JH band with those derived from the individual positions given by GAIA DR2 gives a maximum deviation of 3.2° for PA and 0.25 arcsec for SEP. Again, these deviations are significantly higher than those reported in our previous work on similar pairs in the optical band (in [11], for example the differences between our measurements and the astrometric values deduced from GAIA DR2 showed an average and standard deviation of only -0.009° / 1.08° and 0.004 arcsec / 0.028 arcsec for PA and SEP respectively). This can probably be attributed, again, to the coarser plate scale but also to the fact that, in our previous work, each reported measurement was computed from several acquisition sequences, each reduced separately, whereas the values used here are computed from a single acquisition sequence.

Concerning photometry, the passband of our filters on the one hand and of GAIA filters on the other hand are too different to allow even an approximate comparaison (and, especially, because GAIA photometry does not extend beyond 1 μm [13]). We are not aware of any data source providing J-band and/or H-band differential magnitudes for binary stars in that range of separation. It is therefore very difficult to assess the accuracy of the ΔM(JH) values reported in Table 2. The only thing we could do was therefore to try drawing some conclusions from the variations of Δm observed when going from our G or R band to the JH one (i.e. from the differences between the values reported in columns 5 or 8 and 11 in Table 2). Indeed, Table 2 shows that the latter is almost systematically lower than the former(s) (with a min/max/mean value of -1.30/0.03/-0.35 for ΔM(JH)-ΔM(G) and -1.5/0.17/-0.31 for ΔM (JH)-ΔM(R). Unfortunately, we were unable to correlate this general trend to the GAIA Teff parameters which, as explained in Section 4, were the best indirect indicator we had of the involved spectral types. The linear correlation coefficient between the measured ΔM (JH) and ΔTeff=Teff2-Teff1, in particular, is very small (0.26). We also tried to correlate ΔM(JH) with other «physically-bound» DR2 parameters such as single Teff values or color indices (BP-RP) without success.

The small size of the data set and our limited knowledge on photomery and astrophysical issues make it difficult to decide whether the previous negative results are due to incorrect measurements (intrinsic accuracy and/or too wide passbands), badly choosen physical indices (with Teff not being a good estimator of the spectral type for instance) or both.

6. Conclusion

The results reported in this paper confirm that observing and measuring visual binary stars in SWIR is

(Text continues on page 579)

† Contrary to pure reflectors, and because of the correcting plate, the position of focus in a Schmidt-Cassegrain telescope depends on the observed wavelength.

†† This computation was carried out using the GDS [11] software.

‡ The GAIA G mag corresponds to a passband going from to 300 to 1000 nm approximately. It therefore should not be confused with the passband of our Astronomik «G» filter.

‡‡As clearly evidenced on the images reproduced in Plate 1. This is a consequence of the classical dependence of the turbulence effects on the wavelength.

Measurements of Visual Binary Stars with a SWIR Camera and a 280 mm Reflector – Part 2

Table 1. Observed Pairs

WDS		GAIA DR2					
ID	NAME	GPA (°)	Gsep (arcsec)	Gmag1	Teff1 (K)	Gmag2	Teff2 (K)
16315+3331	BU 816	221.1	5.04	7.08	7982	11.48	5172
16492+4559	BU 627A,BC	42.4	2.11	4.80	8974	8.29	5096
16530+4045	A 1868	302.3	2.13	9.46	5069	9.82	4707
17344+1310	A 2184AB	31.4	1.93	7.22	7412	10.20	5287
17561+2130	STT 339	170.0	4.19	8.13	5806	10.40	4774
17564+1820	STF2245BA	111.9	2.64	7.14	5038	7.39	9554
17571+4551	HU 235	286.2	1.59	6.70	6268	8.91	5096
18222+1126	STF2311AB	86.7	3.03	9.19	4802	9.49	3813
18338+1744	STF2339AB,CD	276.6	1.55	7.30	6876	8.69	5096
18443+3940	STF2382AB	346.1	2.29	4.95	8400	6.02	6497

Table 2. Measurements

ID	Date	G			R			JH			NOTE
		PA (°)	SEP (arcsec)	ΔM	PA (°)	SEP (arcsec)	ΔM	PA (°)	SEP (arcsec)	ΔM	
16315+3331	2018.484	219.4	5.11	5.2	220.9	5.03	4.5	219.5	5.35	4.1	1
16492+4559	2018.495	43.6	2.22	2.3	n/a	n/a	n/a	42.0	1.96	2.4	2
16530+4045	2018.484	303.3	2.27	2.3	303.8	2.38	2.5	304.4	2.06	1.0	3
17344+1310	2018.495	41.0	1.64	2.3	34.2	1.82	2.3	31.3	1.88	2.4	4
17561+2130	2018.484	168.0	4.26	2.5	169.4	4.20	2.5	169.4	4.21	2.1	
17564+1820	2018.495	112.5	2.52	2.0	112.3	2.45	1.7	112.5	2.60	1.9	5
17571+4551	2018.495	285.1	1.85	2.2	289.4	1.82	2.4	286.8	1.60	2.0	6
18222+1126	2018.484	264.4	3.08	1.4	265.1	3.09	1.3	264.4	3.06	1.1	7
18338+1744	2018.495	274.1	1.63	1.1	275.9	1.46	1.2	277.4	1.69	1.1	
18443+3940	2018.495	346.3	2.22	0.8	345.1	2.21	0.8	345.1	2.25	0.8	8

Notes for Table 2

1. B faint on G image. Large ΔM
2. G image slightly elongated due to imperfect ADC setting. Companion not detected on R image
3. Companion significantly brighter on J image
4. G image imperfectly reconstructed
5. J image slightly elongated
6. Companion on first diffraction ring
7. Artefact on all images due to imperfect bispectrum-based reconstruction
8. ε1 Lyrae

Table 3 – O-C residuals for pairs having a known orbit

NAME	WDS ID	DATE	O-C PA (°)	O-C SEP (")	GRADE	REF
BU 627A,BC	16492+4559	2018.495	1.95	-0.145	5	Fmr2012a
STF2382AB	16492+4559	2018.495	0.33	0.022	4	Nov2006e

Measurements of Visual Binary Stars with a SWIR Camera and a 280 mm Reflector – Part 2

(Continued from page 577)

technically feasible by amateurs with a relatively modest equipment (there are now several companies selling small SWIR cameras at affordable prices). To the best of our knowledge this is the first time that a combination of SWIR imaging and speckle-based reduction techniques are used in the amateur field.

The best usage of such observations, however, should be carefully thought of. Photometric issues, in particular, should be investigated to see whether differential magnitude measurements in J and/or H bands can really help the determination of spectral types.

As already stated in our first paper on this subject, the systematic search of companions of late (M) spectral types which could have be been left uncovered by optical surveys such as GAIA is also a interesting application of the instrumental techniques described here.

7. Acknowledgments

This research has made use of the Washington Double Star and 6th Orbit catalogs maintained at the U.S. Naval Observatory and of data from the European Space Agency (ESA) mission Gaia (www.cosmos.esa.int/gaia), processed by the Gaia Data Processing and Analysis Consortium [10]. Data reduction was carried out using the Reduc software developed and maintained by F. Losse and the SpeckleToolbox software developed and maintained by D. Rowe. We have been using the Owl 640 camera courtesy of J.E. Communal (Raptor Photonics)

8. References

[1] Sérot, J., "Measurements of Visual Binaries with M-Type Companions with a SWIR Camera and a 280 mm Reflector', *JDSO*, **14**(1), 78-82, 2018.

[2] Sérot, J., "Measurements of Aitken Visual Binary Stars: 2017 Report", *JDSO*, **14**(3), 527-537, 2018.

[3] Sérot, J., Wasson, R., Rowe, D., Genet, R., "Bispectrum-based Measurements of Close Large-Differential Magnitude Visual Double Stars", *JDSO*, **14**(4), 711-727, 2018.

[4] http://www.raptorphotonics.com/products/owl-640-cameralink-stabilized

[5] http://genicapture.com

[6] Harshaw, R., R., Rowe, D., Genet, R., "The Speckle Toolbox: A Powerful Data Reduction Tool", *JDSO*, **13**(1), pp 52-67, 2017.

[7] Losse, F. Reduc, v5.0. http://www.astrosurf.com/hfosaf

[8] Sérot, J., "Measurements of Aitken Visual Binary Stars: 2018 Report", *JDSO*, **15**(3), 315-321, 2019.

[9] Mason, D.B., Wycoff, G.L., Hartkopf, W.I., "Washington Double Star Catalog", USNO, 2015. http://www.usno.navy.mil/USNO/astrometry/optical-IR-prod/wds/WDS

[10] www.cosmos.esa.int/web/gaia/dpac/consortium

[11] Sérot, J., "Measurements of 121 New Visual Binary Stars Suggested by the Gaia Data Release 2", *JDSO*, **15**(2), 287-296, 2019.

[12] Hartkopf, W.I., Mason, D.B., "Sixth Catalog of Orbits of Visual Binary Stars", USNO, 2009. http://www.usno.navy.mil/USNO/astrometry/optical-IR-prod/wds/orb6

[13] https://www.cosmos.esa.int/web/gaia/iow_20180316

Plate 1 begins on the next page.

Measurements of Visual Binary Stars with a SWIR Camera and a 280 mm Reflector – Part 2

Plate 1. Post-Reduction Images

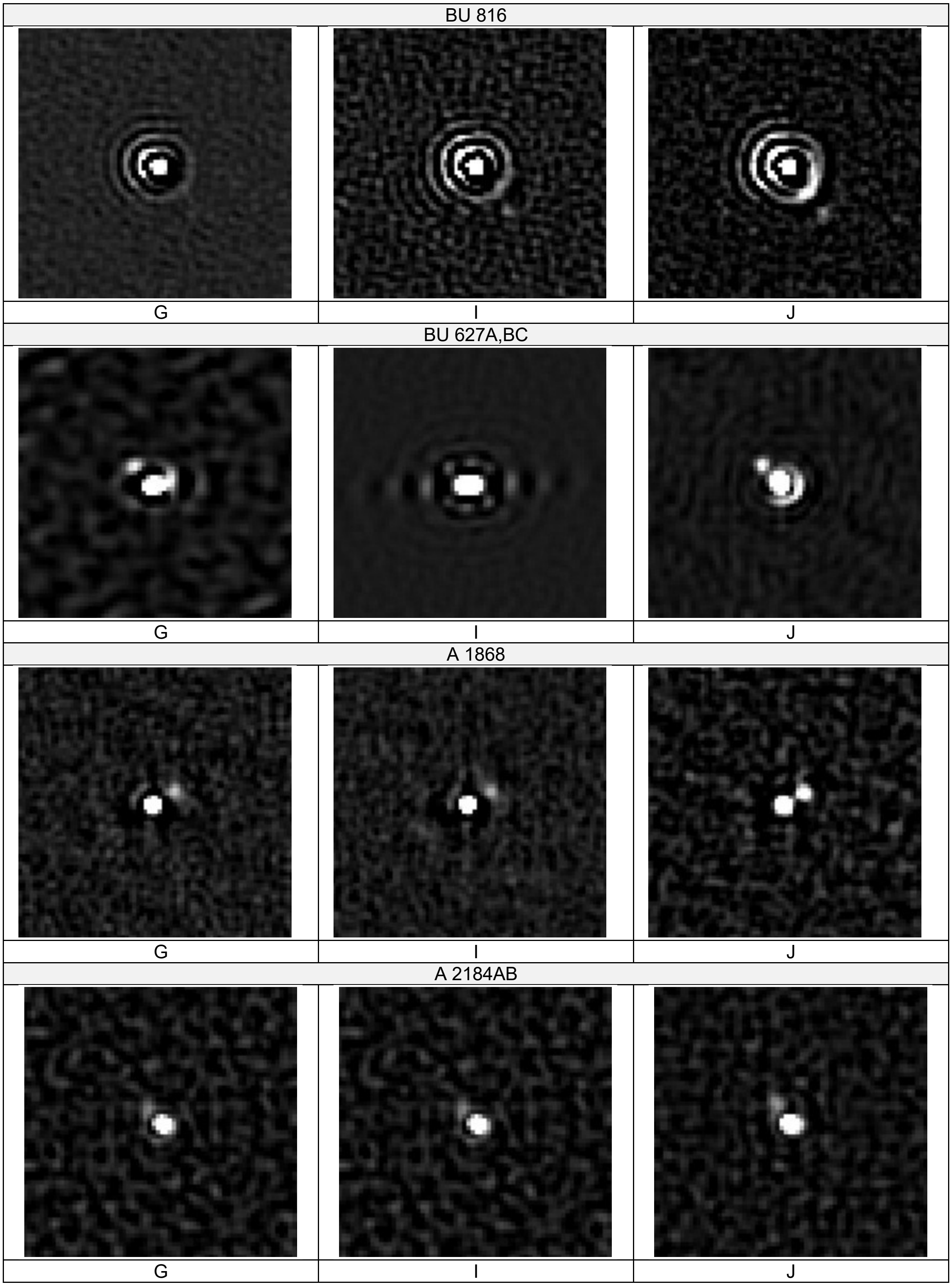

Measurements of Visual Binary Stars with a SWIR Camera and a 280 mm Reflector – Part 2

Plate 1 (continued). Post-Reduction Images

STT 339		
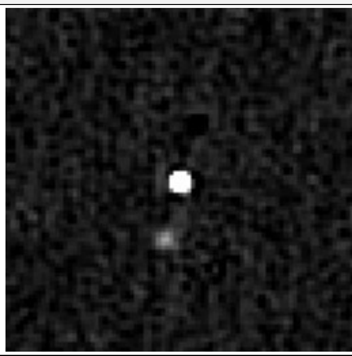	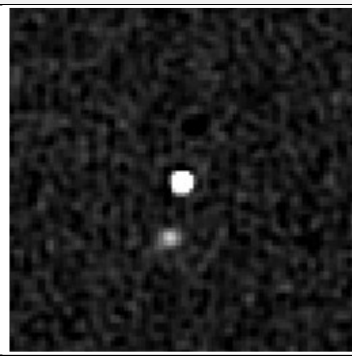	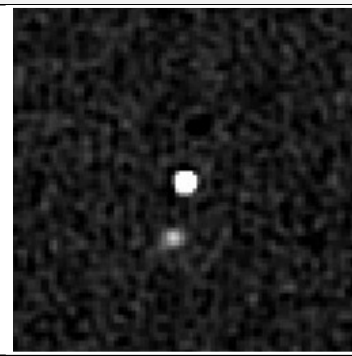
G	I	J
STF2245BA		
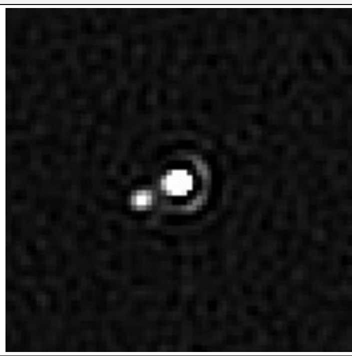	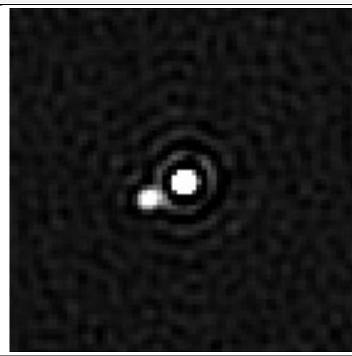	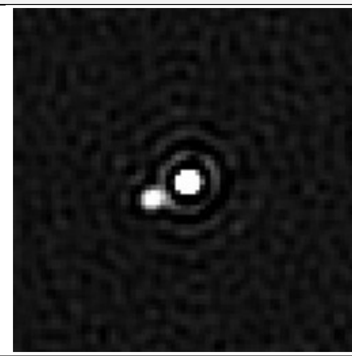
G	I	J
HU 235		
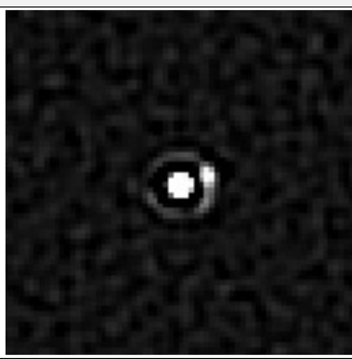	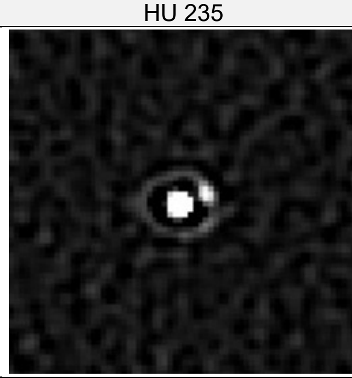	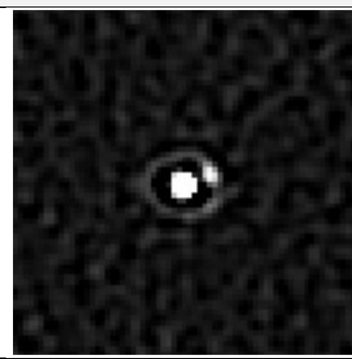
G	I	J
STF2311AB		
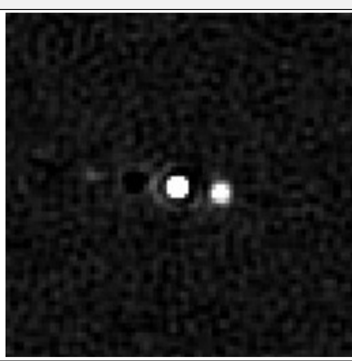	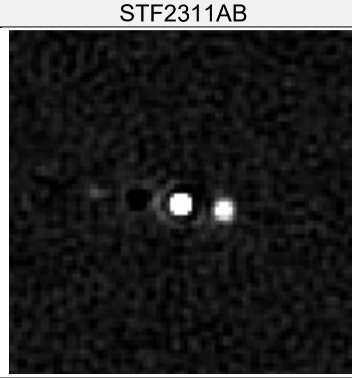	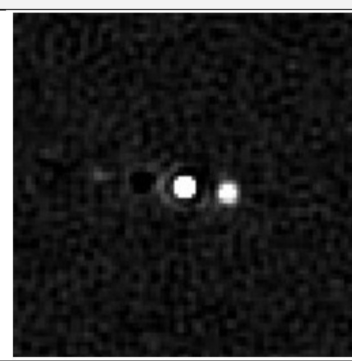
G	I	J

Measurements of Visual Binary Stars with a SWIR Camera and a 280 mm Reflector – Part 2

Plate 1 (conclusion). Post-Reduction Images